Numerical Investigation of Stiffness Properties of FDM Parts as a Function of Raster Orientation

Sanchita Sheth[*], Robert M. Taylor [†]
University of Texas at Arlington, Arlington, TX, 76019

Hari Adluru [‡]
University of Texas at Arlington Research Institute, Arlington, TX, 76019

This work discusses a numerical investigation of stiffness properties of parts printed using Fused Deposition Modeling (FDM). Small volumes of different raster orientations were modelled and meshed using SIMULIA™ (Abaqus). These meshes were exported to a damage prediction software BSAM, which uses a homogenization approach to model interface bond strength between adjacent raster beads. In BSAM, boundary conditions, connectivity and material properties have been specified. This BSAM model was then used to compare stiffness properties at various raster angles. A similar trend in the modulus values was observed from experimental test data. Further this model could be used to specify and predict interface properties for the specimens at various raster angles which could be used to eventually predict strength and fracture.

I. Introduction

Additive manufacturing (AM) has great potential to significantly expand design freedom for a wide range of applications. This design freedom is currently being realized in many non-critical, lightly loaded applications. However, most potential applications require reliable material characterization to ensure a design performs within its design environment, limit, and life requirements.

In polymer Fused Deposition Modeling (FDM) AM, the layered fabrication process that enables this expanded design freedom also creates a discontinuous material with strongly directional mechanical properties, numerous fracture interfaces and stress singularities, and severely degraded fatigue life. The severity of the fabrication process effect on bulk material capability depends heavily on process parameters and local geometry. Consequently, methods to accurately characterize and predict mechanical behavior considering process parameters and local geometry are needed.

This paper discusses an investigation of raster angle dependency of stiffness properties of polymer parts printed using Fused Deposition Modeling (FDM). The work builds on previous work by Osborn, et al,[1] that examined anisotropic mechanical properties of individual FDM layers using classical laminated plate theory and homogenization techniques. Using this methodology, the current work examines raster angle effects on stiffness and compares the computational results to an experimental investigation of raster orientation.[2]

II. Background

A. FDM Additive Manufacturing

In the FDM process, a flexible filament is heated to a glassy state and extruded through a controlled deposition head onto a build plate in order to build the part layer by layer vertically. Within a layer, cross-sectional geometry is deposited first in one or more contour beads to define boundaries and then an infill, which may be a solid raster or a porous pattern. Material continuity within a part is developed as contour beads are deposited in adjacent roads and bonding takes place via diffusion welding. Part stiffness and strength therefore is a strong function of the developed

[*]Graduate Masters Student, University of Texas at Arlington
[†] Professor in Practice, University of Texas at Arlington
[‡] Post-Doctoral Fellow, University of Texas at Arlington Research Institute

inter-bead bond strength, contact area, gaps and voids as well as bead shape and orientation with respect to loading direction. These dependencies lead to anisotropic mechanical behavior within materials and parts built using FDM.

This anisotropic mechanical behavior of FDM printed materials has received significant attention in recent years and work has been performed to address the effects of FDM build parameters on stiffness, strength, fatigue, fracture, and creep. Much of the basic tensile testing follows standard the ASTM D638 test method for tensile properties of plastics[3] and examines process parameter effects on the resulting properties. Ahn et al[4] examined raster orientation, air gap, bead width, color, and model temperature effects on tensile and compressive strengths of directionally fabricated specimens. Bellini and Guceri[5] developed an anisotropic FDM stiffness matrix from filament testing. Riddick et al[6] executed tensile testing to study the effect of process-induced anisotropy on the mechanical response. Ziemian et al[7] executed tension, compression, 3-point bend, and tension-tension fatigue testing to characterize the anisotropic mechanical properties of ABS FDM parts, showing a strong sensitivity to raster angle and quantity of air gaps between rasters. They performed further investigations[8] and noted tensile behavior is improved by aligning the fibers of unidirectional laminae more closely with the axis of the applied stress and tensile and fatigue performance improved with alternating laminae θ°/(θ-90°). Lee and Huang[9] performed experimental fatigue investigation on FDM ABS as a function of build orientation. Afrose et al[10] performed a similar investigation of build orientation effect on fatigue behavior of FDM PLA. Zhang[11] executed tension, creep, and fatigue testing and laminate-based finite element modeling to study mechanical property sensitivity to build orientation. Motaparti[12] executed flexural and compression testing of ULTEM 9085 to study the individual and combined effects of build direction, raster angle, and air gap (sparse infill) build parameters on flexural and compressive stiffness and strength properties. Torrado and Roberson[13] examined tensile specimen failure and evaluated anisotropy versus geometry and raster pattern. Huang and Singamneni [14]applied experimental and analytical models of raster angle effects on modulus and strength in FDM parts. Rezayat et al[15], developed finite element models at multiple length scales and compared results with experimental full field strain data for different raster angles and filament gaps. Patel et al[16] performed experimental investigation of fracture of FDM printed ABS for different crack length and layer of orientations.

Some researchers have developed methods to optimize mechanical properties. Ulu, et al[17] developed an optimization method to enhance structural performance through build orientation optimization that recognizes these mechanical property sensitivities. Torres et al[18] likewise developed an approach for optimizing FDM part mechanical properties based on experimentally determined sensitivities to build parameters, which included layer thickness, density or infill percentage, extrusion temperature, speed, infill direction and component orientation.

Many researchers have shown and validated applications laminated plate theory used in composite materials to describe mechanical behavior in FDM printed materials. El-Gizawy, et al[19] studied process-induced properties of FDM printed ULTEM 9085 using classical laminated plate theory to determine the anisotropic stiffness matrix and thereby establish constitutive relationships that predict the internal structure of FDM materials. The authors validated the approach with tensile testing and finite element correlation. Li et al[20] performed theoretical and experimental analyses of mechanical properties of FDM processes and prototypes to develop constitutive models and equations to determine the elastic constants of FDM printed materials. Sayre[21] modeled FDM printed materials as a layered composite with modified properties to account for imperfect bonding between layers. Rodriguez et al[22], obtained effective elastic moduli using a strength of materials and elasticity approach based on the asymptotic theory of homogenization and experimentally validated predicted properties.

Finally, much work has been performed to characterize mechanical property degradation due to FDM process characteristics. Park and Rosen[23] addressed mechanical property degradation in cellular materials due to bounding surface errors using as-fabricated voxel modeling and a discrete homogenization approach. Baikerikar[24] examined mechanical properties for a variety of infill patterns, comparing finite element simulations and experimental results for tensile dogbone specimens. Faes et al[25] executed testing to study the influence of interlayer cooling time, which affects the coalescence of the interconnection between adjacent tracks and layers, on quasi-static properties.

B. Finite Element Method using BSAM

BSAM is a computational structural analysis software developed by University of Dayton Research Institute in collaboration with the Air Force Research Laboratory, WPAFB, OH and NASA Langley Research Center, Hampton, VA.[26] It was initially developed to provide accurate stresses analysis in multilayered composite materials and further expanded for progressive failure analysis under static and fatigue loading. Discrete Damage Modelling (DDM) based on Regularized eXtended Finite Element Method (Rx-FEM) was developed for this purpose.[27,28,29]

The scope of current work is limited to determining elastic moduli, which is based homogenization approach.[30] The homogenization method implemented in BSAM is tailored to resolve field behavior across regions where there is abrupt variation in the local microgeometry. The numerical method developed in BSAM is a fast way to extract

local field information inside prescribed subdomains without having to resort to a full numerical simulation. The homogenized method used for local field assessment is explained in detail by Breitzman et al.[27] Even though the authors discussed the homogenization formulas for prestressed and/or thermomechanical loads, they can be simplified for a composite body having no initial stress.

Let a composite body be subjected to an external force f. Let u^{ε} and σ^{ε} be the displacements and stresses associated with this force. Based on the homogenization procedure the asymptotic expansions for displacements u^{ε} and stresses $\sigma_{ij}^{\varepsilon}$ are

$$\boldsymbol{u}^{\varepsilon} = \boldsymbol{u}^{(0)}(\boldsymbol{X}) + \varepsilon \boldsymbol{u}^{(1)}(\boldsymbol{X},\boldsymbol{Y}) + \cdots \quad (1)$$

$$= \boldsymbol{u}^{(0)}(\boldsymbol{X}) + \sum_{k=1}^{\infty} \varepsilon^{k} \boldsymbol{u}^{(k)}(\boldsymbol{X},\boldsymbol{Y}) \quad (1)$$

$$\sigma_{ij}^{\varepsilon} = \sum_{k=0}^{\infty} \varepsilon^{k} \sigma_{ij}^{(k)}(\boldsymbol{X},\boldsymbol{Y}) \quad (2)$$

Here X are 'slow' variables, and Y = X/ε are the 'fast' variables and ε- is the characteristic size of the microstructure. Here the functions on the right side are assumed to be periodic in Y within the periodicity cell. The differential operators are represented in the form of sum of operators in X and Y by using the two-scale expansion shown in equations (1) & (2) above.

The current FDM specimens are distinguished by the presence of local periodic microstructure. In order to capture this local material heterogeneity, some form of local enhancement of approximation space is required to accurately estimate the sub structural (ply level) units.

III. Methodology for Stiffness Calculation

In this work, a finite element representative volume cell approach is used to calculate stiffness at various 3D print raster angles. FDM bead geometric modeling, the representative volume cell approach, and stiffness calculations are discussed below.

A. FDM Bead Geometry

Osborn et al.,[1] in their work 3D-printed unidirectional section specimens of ULTEM 9085 on a FORTUS 400MC. These specimens were cut normal to the raster orientations and cross-sectional photomicrographs were obtained. The cross-sectional dimensions of a single bead were obtained from the photomicrographs. These dimensions were used to create the bead geometry as shown in Figure 1.

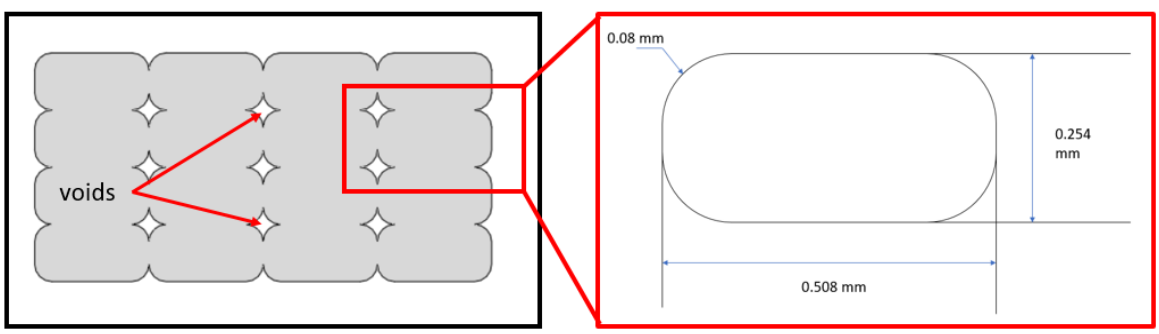

Figure 1 - Cross Section of Bead

B. Representative Volume Cell (RVC)

A Representative Volume Cell (RVC) was built using Abaqus/CAE 2016 based on the cross-section images. As shown in Figure 2, for the 0° raster orientation, this volume consisted of 4 layers of roads. Each layer consisted of 4 roads. The RVC chosen is more than that required for stiffness property computation and is considered for future predictions of both failure and fracture strengths.

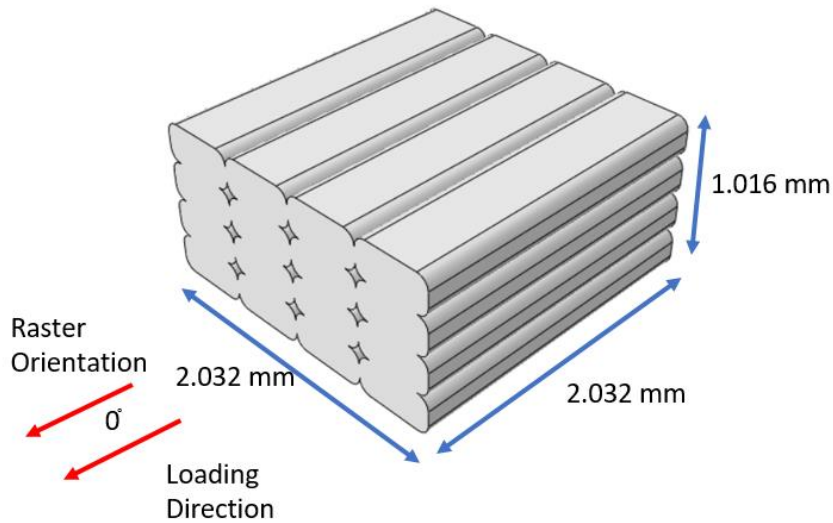

Figure 2 - 0° Representative volume cell

RVCs of the same dimensions were built for different raster orientations such as 15°, 30°, 45° and 90° as shown in Figure 3. Preprocessing operations like building the 3D geometry and meshing were performed using Abaqus/CAE 2016. An input file was generated to be imported into the BSAM Export Module. Displacement boundary condition is applied along 1-1 direction (x axis), which represent the tensile loading on the RVC. The displacement on the external boundary is given by

$$u_i = \overline{\varepsilon}_{ij}\, x_j \tag{3}$$

where $\overline{\varepsilon}_{ij}$ is observer strain, which in the present case is not equal to the volume average strain due to presence of voids.[1] Therefore, instead of direct computation of average strain, the observer strain is used. In all cases these strain values are incremented uniformly to a maximum value of 0.01. The above equation is used to assign displacement boundary conditions for all the raster orientations. The volume average stress is given by

$$\overline{\sigma}_i = \frac{1}{V}\int_V \sigma_i \, dV \tag{4}$$

The homogenized compliance matrix is computed as

$$\overline{S_i} = [\overline{\sigma_i}]^{-1}\overline{\varepsilon_i} \tag{5}$$

followed by calculation of Young's moduli using standard formulae.[1]

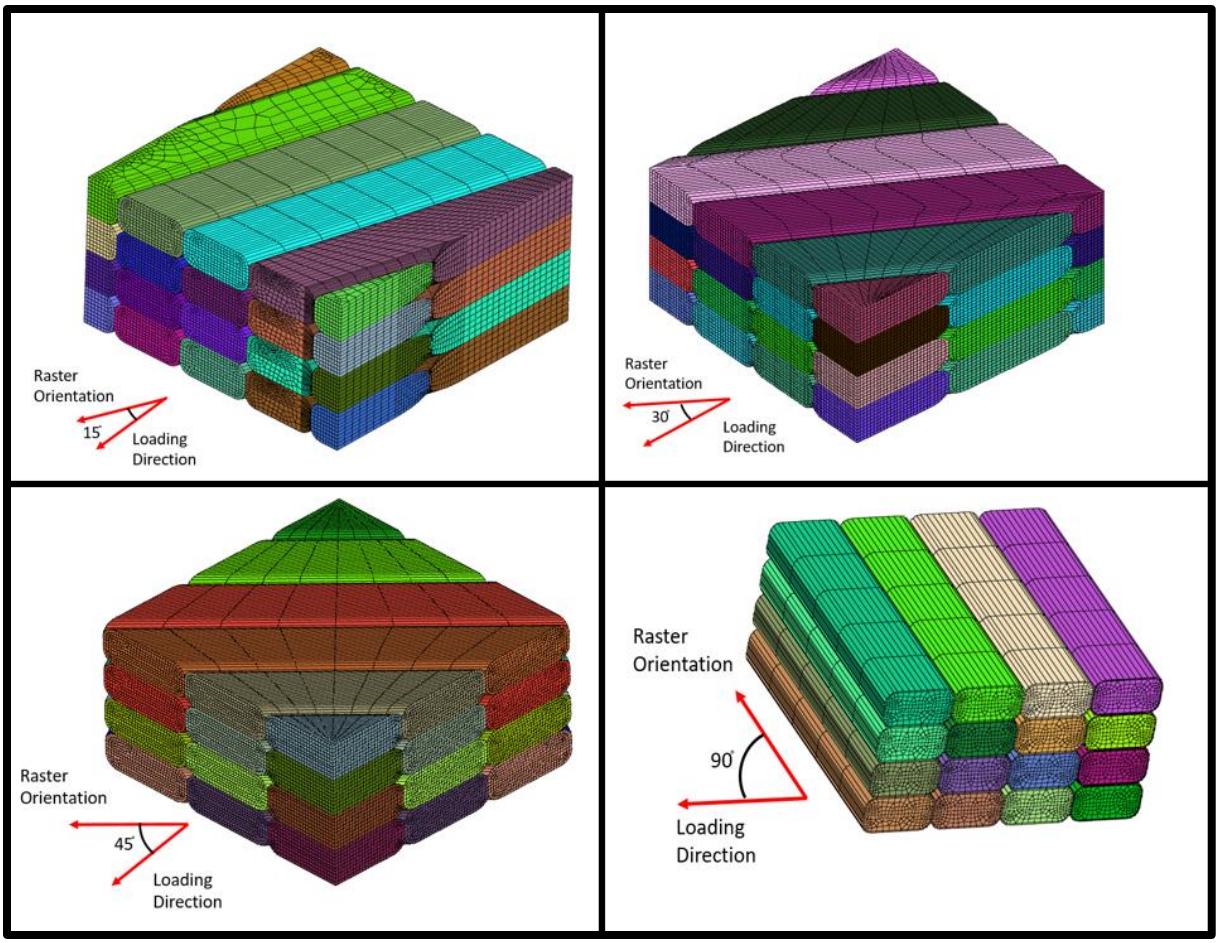

Figure 3 - Meshed RVCs for various orientations

C. Stiffness Calculation

To determine stiffness properties, in the BSAM export module, static displacement boundary conditions were applied to the RVC. One face of the RVC was fixed in x, y and z and on the opposite face, a displacement boundary condition of 0.1 mm was applied in slow increments. The application of the displacement boundary condition was done in steps of 1% of the total load. Next, the material file was imported into the BSAM export module. The model was then exported as a BSAM input file. The file was run in the BSAM software and outputs for displacement, force, stress and strain were generated at each step. The stiffness of the RVC was calculated from the stress and strain values.

IV. Results

Using the previously described methodology, results have been obtained for displacement and stiffness and compared to test data as discussed below.

A. Displacement

Displacement was applied in steps of 1% of total load. So, at each step, a displacement of 0.001 mm was applied. Figure 4 shows the displacement plot at the 10th load step for the 0° orientation. Here, the displacement value at the load end is 0.01 mm. Figure 4 (b) shows the displacement plot at the 20th load step for the 30° orientation. Here, the displacement value at the load end is 0.02 mm

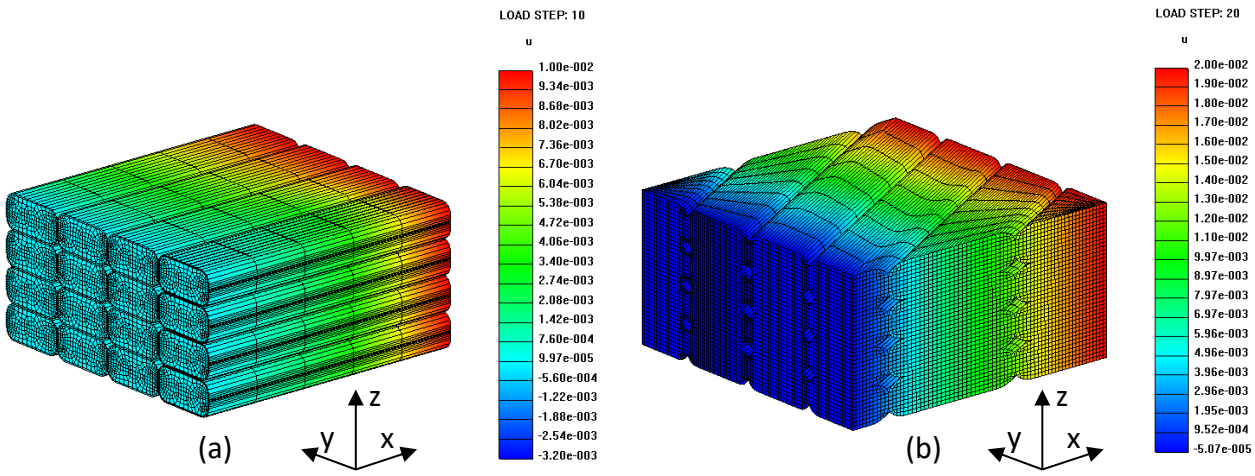

Figure 4 – (a) 0° Displacement plot at 10th load step (b) 30° Displacement plot at 20th load step

B. Stiffness

On observing the stress distribution near the voids in Figure 5, peak stresses at the stress concentrations were within the linear range of the material. Hence, the material was considered to be a linear elastic material. Stiffness values for different raster orientations were calculated and compared to values obtained from the experimental test data. Table 1 lists the BSAM and Experimental values. As observed in Table 1, the stiffness values decrease from 0° to 45° raster orientations and then increase from 45° to 90° orientations.

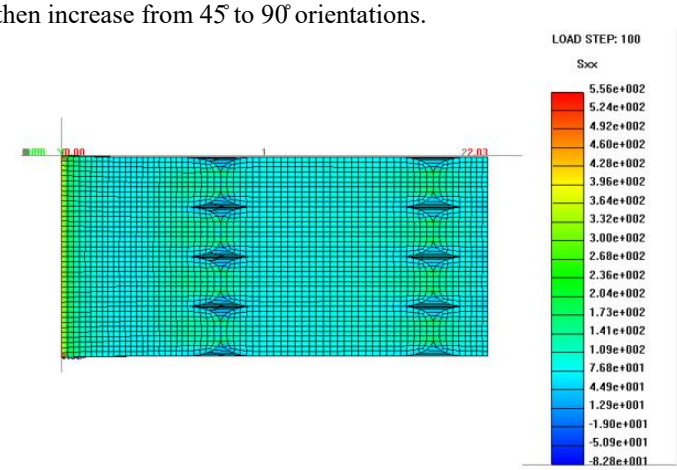

Figure 5 - Stress distribution near voids

Table 1 - Stiffness Values

Raster Orientation (Degree)	BSAM Calculated Modulus (MPa)	Modulus from Test Data (MPa)[§]
0	2334.14	2369.64
15	2281.33	2277.83
30	2264.41	2161.90
45	2230.35	2046.10
90	2302.51	2212.14

[§] Calculated as average of number of specimens per raster orientation

C. Stiffness Comparison

Modulus values were calculated by tensile tests performed by Khatri[2] on two sets of tensile specimens with different raster orientations. These experimental values were compared with values obtained from BSAM. As observed in Figure 6, the stiffness values decrease from 0° to 45° raster orientations and then increase from 45° to 90° orientations. The experimental values show a similar trend as the values obtained numerically.

As observed in Figure 6, the BSAM modulus values obtained for raster orientations 30º and 45º are higher than the experimental values. Such variations could be a result of non-linearity, stress concentration, varying local geometry and machine settings. The current work models the specimens in as-designed condition. To capture the variations, there is a need to model the specimens in as-built condition. The local geometry could be viewed using CT scan technology and accordingly an as-built model could be generated.

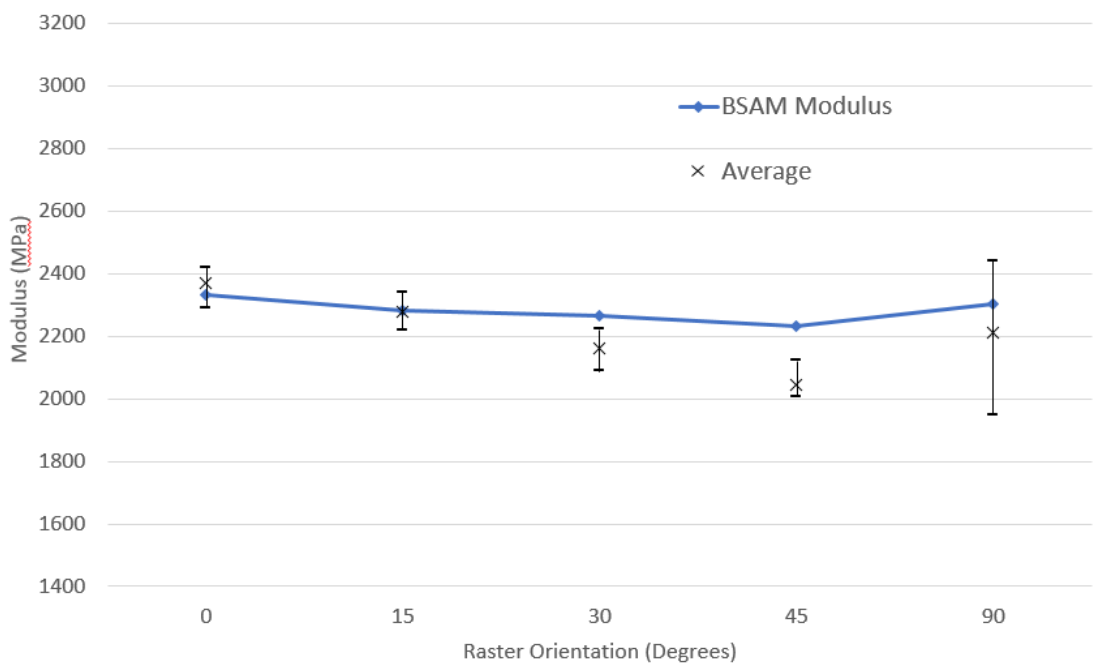

Figure 6 - Comparison of Experimental and BSAM calculated Modulus Values

V. Conclusion

A. Summary of Work and Results

This work presents a procedure for numerically predicting the Elastic Modulus of FDM printed parts as a function of raster angle. In this work, 0, 15, 30, 45, 90 degree FDM raster orientations were modeled and meshed using ABAQUS and the Elastic Modulus values for these orientations were numerically predicted using BSAM. These modulus values were observed to decrease from 0° to 45° and then increase from 45° to 90°. These values show a similar trend when compared to experimental testing data.

B. Future Work

Future work is planned to build on the current stiffness results presented here. The next step will be to predict the strength of FDM printed parts as a function of the void geometry, which is a function of the raster angle as shown in Figure 7. Also, BSAM will be used to predict fracture of the FDM printed parts. The current work uses 'as-designed' geometry to model the specimens. Another approach would be to use the 'as-built' geometry to model the specimens. This geometry will be obtained by CT scan technology. A mesh sensitivity study will also be performed to determine the optimum mesh size.

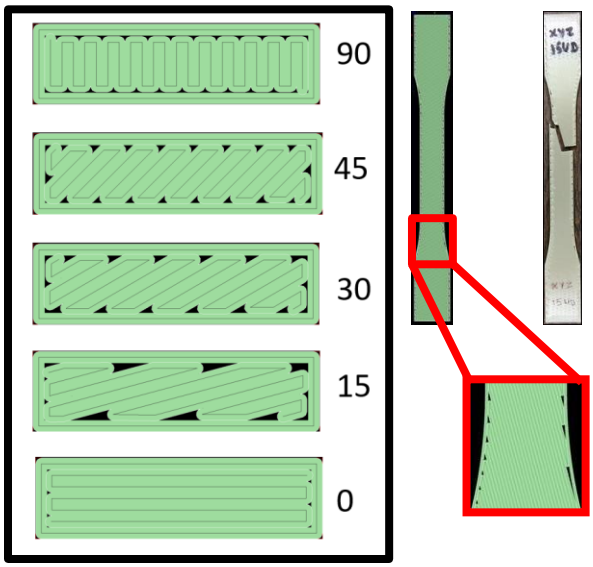

Figure 7 - Void geometry due to raster angle

VI. Acknowledgements

The authors thank The Composites Performance Research Team AFRL\RXCC at the US Air Force Research Labs (Wright Patterson AFB, Dayton, OH), especially Dr. Endel V. Iarve and Dr. Lauren Ferguson for providing the required BSAM\VTMS software and technical support.

Static tensile test data referenced in Figure 6 was generated under contract to Stratasys, Inc. in support of America Makes *Design Guidance for Additive Manufacturing*, Fall 2016.

VII. References

[1] T. Osborn, E. Zhou, R. Gerseski, D. Mollenhauer, G.P. Tandon, T.J. Whitney, and E.V. Iarve, "Experimental and Theoretical Evaluation of Stiffness Properties of Fused Deposition Modeling Parts," *American Society of Composites-30th Technical Conference*. 2015.

[2] Khatri, Amit. *Effect of Manufacturing-Induced Defects and Orientation on the Failure and Fracture Mechanism of 3d Printed Structures*, Master's Thesis, University of Texas at Arlington, 2016.

[3] ASTM Standard D638 - 10. (2010). *Standard Test Method for Tensile Properties of Plastics*. ASTM International, West Conshohocken, Pennsylvania, DOI: 10.1520/D0638-10.

[4] S. H. Ahn, M. Montero, D. Odell, S. Roundy, P. K. Wright, "Anisotropic Material Properties of Fused Deposition Modeling ABS", *Rapid Prototyping*, 8(4) (2002) 248-257.

[5] Bellini, Anna, and Selçuk Güçeri. "Mechanical Characterization of Parts Fabricated Using Fused Deposition Modeling." *Rapid Prototyping Journal* 9.4 (2003): 252-264.

[6] Jaret Riddick, Asha Hall, Mulugeta Haile, Ray Von Wahlde, Daniel Cole, and Stephen Biggs, "Effect of Manufacturing Parameters on Failure in Acrylonitrile-butadiane-styrene Fabricated by Fused Deposition Modeling." *Proceedings of the 53rd AIAA/ASME/ASCE/AHS/ASC Structures, Structural Dynamics and Materials Conference*, Honolulu, HI, 2012.

[7] Ziemian, Constance, Mala Sharma, and Sophia Ziemian. "Anisotropic Mechanical Properties of ABS Parts Fabricated by Fused Deposition Modelling." in *Mechanical Engineering*, Murat Gokcek (Ed.),InTech, 2012.

[8] Ziemian, Sophia, Maryvivian Okwara, and Constance Wilkens Ziemian. "Tensile and Fatigue Behavior of Layered Acrylonitrile Butadiene Styrene." Rapid Prototyping Journal 21.3 (2015): 270-278.

[9] Lee, John, and Adam Huang. "Fatigue Analysis of FDM Materials." *Rapid Prototyping Journal* 19.4 (2013): 291-299.

[10] Afrose, M. F., Masood, S. H., Iovenitti, P., Nikzad, M., & Sbarski, I. "Effects of Part Build Orientations on Fatigue Behaviour of FDM-processed PLA Material." *Progress in Additive Manufacturing* 1.1-2 (2016): 21-28.

[11] Zhang, Hanyin. *Characterization of Tensile, Creep, and Fatigue Properties of 3D Printed Acrylonitrile Butadiene Styrene*. Master's Thesis, Purdue University Indianapolis. 2016.
[12] Motaparti, Krishna Prasanth. *Effect of Build Parameters on Mechanical Properties of Ultem 9085 Parts by Fused Deposition Modeling*. Master's Thesis, Missouri University of Science and Technology, 2016.
[13] Torrado, Angel R., and David A. Roberson. "Failure Analysis and Anisotropy Evaluation of 3D-printed Tensile Test Specimens of Different Geometries and Print Raster Patterns." *Journal of Failure Analysis and Prevention* 16.1 (2016): 154-164.
[14] Huang, Bin, and Sarat Singamneni. "Raster Angle Mechanics in Fused Deposition Modelling." *Journal of Composite Materials* 49.3 (2015): 363-383.
[15] Rezayat, H., Zhou, W., Siriruk, A., Penumadu, D., & Babu, S. S. "Structure–mechanical Property Relationship in Fused Deposition Modelling." *Materials Science and Technology* 31.8 (2015): 895-903.
[16] Ravi Patel, H.N.Shah, Susheela V. Kumari, "Experimental Investigation of Fracture of ABS Material by ASTM D-5045 for Different Crack Length & Layer of Orientation Using FDM Process," *International Journal of Mechanical and Industrial Technology*, Vol. 3, Issue 1, (2015):79-83.
[17] Ulu, Erva, et al. "Enhancing the Structural Performance of Additively Manufactured Objects Through Build Orientation Optimization." *Journal of Mechanical Design* 137.11 (2015): 111410.
[18] Torres, Jonathan, Jonathan Torres, Matthew Cole, Matthew Cole, Allen Owji, Allen Owji, Zachary DeMastry, Zachary DeMastry, Ali P. Gordon, and Ali P. Gordon, "An approach for mechanical property optimization of fused deposition modeling with polylactic acid via design of experiments." *Rapid Prototyping Journal* 22.2 (2016): 387-404.
[19] El-Gizawy, A. Sherif, Shan Corl, and Brian Graybill. "Process-induced Properties of FDM Products." *Proceedings of the ICMET*, International Conference on Mechanical Engineerings and Technology Congress & Exposition. 2011.
[20] Li, Longmei, Qiao Sun, Celine Bellehumeur, and Peihua Gu. "Composite Modeling and Analysis for Fabrication of FDM Prototypes with Locally Controlled Properties." *Journal of Manufacturing Processes* 4.2 (2002): 129-141.
[21] Sayre III, Robert. *A Comparative Finite Element Stress Analysis of Isotropic and Fusion Deposited 3D Printed Polymer*. Master's Thesis, Rensselaer Polytechnic Institute Hartford, (2014).
[22] Rodríguez, José F., James P. Thomas, and John E. Renaud. "Mechanical Behavior of Acrylonitrile Butadiene Styrene Fused Deposition Materials Modeling." *Rapid Prototyping Journal* 9.4 (2003): 219-230.
[23] Park, Sang-in, and David W. Rosen. "Quantifying Mechanical Property Degradation of Cellular Material Using As-fabricated Voxel Modeling for the Material Extrusion Process." *Proceedings of the Annual Solid Freeform Fabrication Symposium*, Austin. 2015.
[24] Baikerikar, Prathamesh. *Comparison of As-built FEA Simulations and Experimental Results for Additively Manufactured Dogbone Geometries*. Master's Thesis, Clemson University, (2017).
[25] Faes, Matthias, Eleonora Ferraris, and David Moens. "Influence of Inter-Layer Cooling Time on the Quasi-static Properties of ABS cComponents Produced via Fused Deposition Modelling." *Procedia CIRP* 42 (2016): 748-753.
[26] Hoos K, Swindeman M, Whitney T, et al. "B-spline analysis method (BSAM)-FE, user manual," *University of Dayton Research Institute*, March 2014.
[27] Iarve, E. V., "Mesh independent modelling of cracks by using higher order shape functions," *International Journal of Numerical Methods in Engineering*, (2003)
[28] Iarve, E. V., Gurvich, M. R., Mollenhauer, D. H., Rose, C. A. and Dávila, C. G., "Mesh-independent matrix cracking and delamination modeling in laminated composites." *International Journal of Numerical Methods in Engineering*, (2011)
[29] Michael J. Swindeman, Endel V. Iarve, Robert A. Brockman, David H. Mollenhauer, and Stephen R. Hallett. "Strength Prediction in Open Hole Composite Laminates by Using Discrete Damage Modeling", *American Institute of Aeronautics and Astronautics Journal*, (2013)
[30] T. D. Breitzman, R. P. Lipton and E. V. Iarve, "Local field assessment inside multiscale composite architectures," *SIAM Journal on Multiscale Modeling & Simulation*, vol. 6, no. 3, pp. 937-962,2007.